PROCEEDINGS A

royalsocietypublishing.org/journal/rspa

Research

Cite this article: Pelinovsky DE, White RE. 2020 Localized structures on librational and rotational travelling waves in the sine-Gordon equation. *Proc. R. Soc. A* **476**: 20200490. http://dx.doi.org/10.1098/rspa.2020.0490

Received: 23 June 2020
Accepted: 24 September 2020

Subject Areas:
differential equations, mathematical physics, wave motion

Keywords:
sine-Gordon equation, librational and rotational waves, rogue waves, kinks and antikinks, Darboux transformation

Author for correspondence:
Dmitry E. Pelinovsky
e-mail: dmpeli@math.mcmaster.ca

Localized structures on librational and rotational travelling waves in the sine-Gordon equation

Dmitry E. Pelinovsky and Robert E. White

Department of Mathematics, McMaster University, Hamilton, Ontario, Canada L8S 4K1

DEP, 0000-0001-5812-440X

We derive exact solutions to the sine-Gordon equation describing localized structures on the background of librational and rotational travelling waves. In the case of librational waves, the exact solution represents a localized spike in space-time coordinates (a rogue wave) that decays to the periodic background algebraically fast. In the case of rotational waves, the exact solution represents a kink propagating on the periodic background and decaying algebraically in the transverse direction to its propagation. These solutions model the universal patterns in the dynamics of fluxon condensates in the semi-classical limit. The different dynamics are related to modulational instability of the librational waves and modulational stability of the rotational waves.

1. Introduction

This paper is inspired by the series of works [1–3] on dynamics of the sine-Gordon equation in the semi-classical limit. This physical regime is relevant for propagation of the magnetic flux along superconducting Josephson junctions [4]. Other physical applications of the sine-Gordon equation include crystal dislocations, DNA double helix, fermions in the quantum field theory and structures in galaxies (see reviews in [5,6]).

The sine-Gordon equation in the semi-classical limit can be written in the form:

$$\epsilon^2 u_{TT} - \epsilon^2 u_{XX} + \sin(u) = 0, \tag{1.1}$$

where the subscripts denote partial derivatives of $u = u(X,T)$ and the parameter ϵ is small. By using the initial data with zero displacement and large velocity, $u(X,0) = 0$ and $\epsilon u_T(X,0) = G(X)$, the authors of [1–3]

THE ROYAL SOCIETY PUBLISHING

studied the sequence $\{\epsilon_N\}_{N\in\mathbb{N}}$ with $\epsilon_N \to 0$ as $N \to \infty$, where ϵ_N is defined from the N-soliton (reflectionless) potential associated with the ϵ-independent velocity profile $G(X)$. The sequence of solutions was termed as *the fluxon condensate*. The regime of rotational waves with $\|G\|_{L^\infty} > 2$ was studied in [1], whereas the regime of librational waves with $\|G\|_{L^\infty} < 2$ was studied recently in [3], the classification corresponds to the dynamics of a pendulum with an angle $\theta = \theta(t)$ satisfying

$$\theta''(t) + \sin(\theta(t)) = 0. \tag{1.2}$$

It was suggested in [2] that the dynamics of fluxon condensates are different between the librational and rotational regimes. In both cases, the initial evolution in the semi-classical limit can be modelled by the travelling wave with slowly varying parameters. Dynamics of librational waves are affected by the gradient catastrophe and the emergence of a universal pattern of rogue waves (localized spikes in space-time on a distributed background) [3]. Dynamics of rotational waves are accompanied by the emergence of a universal pattern of propagating kinks and antikinks at the interface between the rotational and librational motion of the fluxon condensate [1].

Figure 1 (reproduced from [2]) shows the dynamics of $\cos(u)$ in the sine-Gordon equation (1.1) with $\epsilon = \epsilon_N$ for $N = 4, 8, 16$. Figure 1*a* shows the regime of librational waves induced by the initial data $u(X, 0) = 0$ and $\epsilon u_T(X, 0) = G(X)$ with $\|G\|_{L^\infty} < 2$. Figure 1*b* shows the regime of rotational waves, for which $\|G\|_{L^\infty} > 2$.

The analysis of [1–3] relies on the reformulation of the Riemann–Hilbert problem used in the integration of the sine-Gordon equation and careful asymptotic estimates. The purpose of our work is *to develop a short and simple algebraic method*, which allows us to construct the exact solutions for the principal waveforms that make dynamics of librational and rotational waves so different. In the case of librational waves, we derive a closed-form solution for a rogue wave decaying algebraically to the periodic background in all directions. In the case of rotational waves, we derive a closed-form solution for propagating kinks and antikinks that decay algebraically to the periodic background in the transverse direction to their propagation. These solutions with localized structures on librational and rotational waves are associated with the particular eigenvalues in the Lax spectrum for which the eigenfunctions are bounded and periodic in space–time coordinates. Since we are not dealing with the initial-value problem in the semi-classical limit, we can scale the space-time coordinates and consider the normalized sine-Gordon equation:

$$u_{tt} - u_{xx} + \sin(u) = 0, \tag{1.3}$$

where $u = u(x, t)$.

Although the algebraic method used for librational and rotational waves is similar, the outcomes are different dynamically. This difference is explained by the different types of spectral stability of the travelling periodic waves [7–9] (see also [10–12] for recent contributions). In the superluminal regime (which is the only regime we are interested in), the librational periodic waves are spectrally unstable and the Floquet–Bloch spectrum forms a figure eight intersecting at the origin. Such instability is usually referred to as modulational instability [7,8]. On the other hand, the rotational periodic waves are modulationally stable in the sense that the only Floquet–Bloch spectrum near the origin is represented by the vertical bands along the purely imaginary axis. The rotational waves are still spectrally unstable in the superluminal regime but the unstable band is given by bubbles away from the origin (see fig. 2 in [7], figs 1–2 in [9], fig. 6 in [10] and fig. 1 in [12]).

We develop the algebraic method that was previously applied to the modified KdV equation in [13,14] and the focusing cubic NLS equation in [15–17]. The travelling periodic waves and the periodic eigenfunctions in space-time coordinates are characterized by using non-linearization of the Lax equations [18]. This method allows us to find particular eigenvalues in the Lax spectrum, for which the first solutions to the Lax equations are bounded and periodic whereas the second, linearly independent solutions are unbounded and non-periodic. When the second solutions of the Lax equations are used in the Darboux transformation, new solutions of

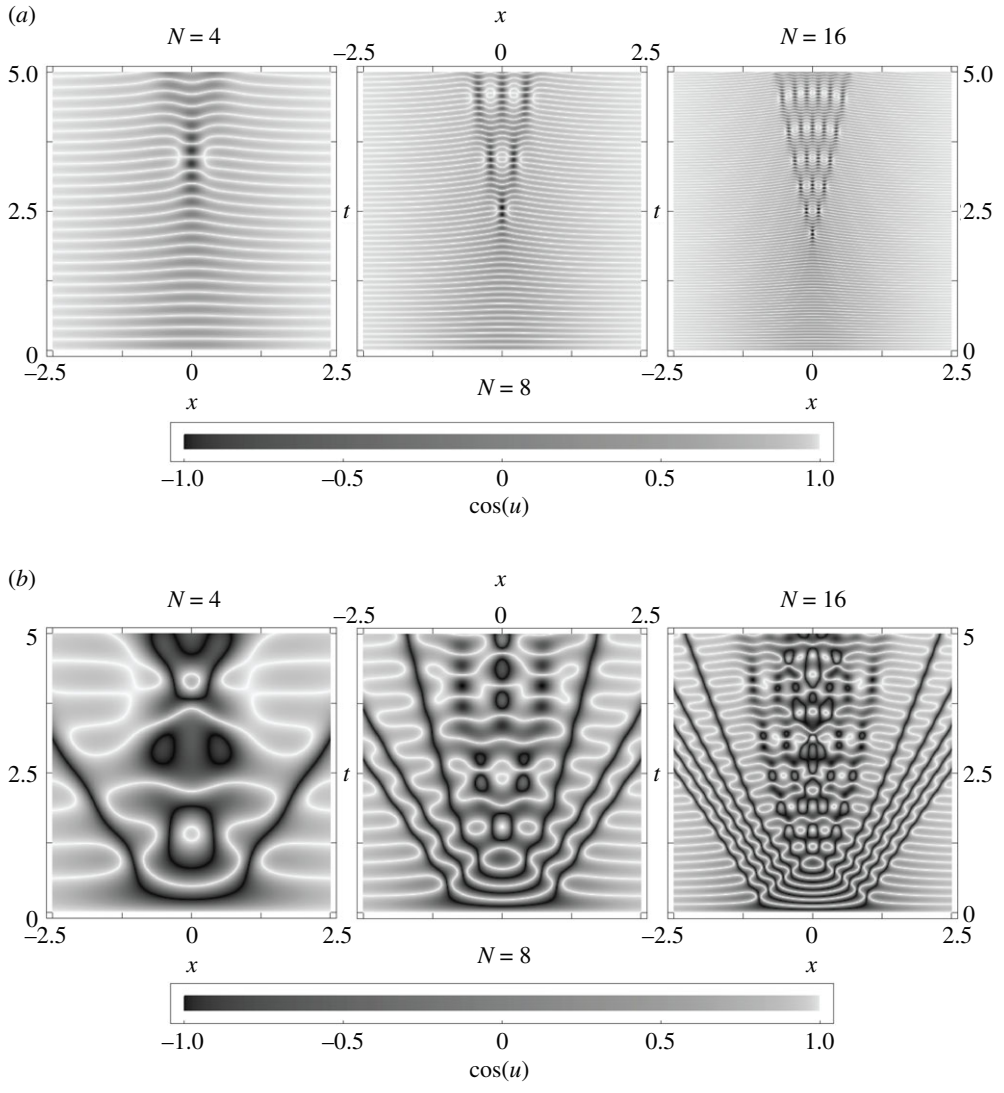

Figure 1. Surface plots of cos(*u*) in space–time coordinates for the dynamics of fluxon condensates in the semi-classical limit. (*a*) Librational waves and (*b*) rotational waves. Reproduced from [2] with permission of the authors.

integrable equations are generated from the travelling periodic wave solutions. The new solutions represent algebraically localized structures on the background of travelling periodic waves. Similar solutions but in a different functional-analytic form were obtained in [19] for the NLS equation and in [20] for the sine-Gordon equation.

The algebraic method can be applied similarly to what was done in [13,14] because the sine-Gordon equation is related to the same Lax spectral problem as the modified KdV, the cubic NLS and other integrable equations considered in the seminal work [21]. In order to enable this application, we have to rewrite the sine-Gordon equation in the characteristic coordinates and use the chain rule for the inverse transformation of variables. We derive explicit expressions for $w := -(u_t + u_x)$ and obtain $\sin(u) = w_t - w_x$ by differentiation. Note that the explicit expressions for w are important for practical applications of extreme waves in self-induced transparency systems [22]. Since the computational details are similar, we will omit many computations and refer to [13,14] or to [23], where computational details can be found.

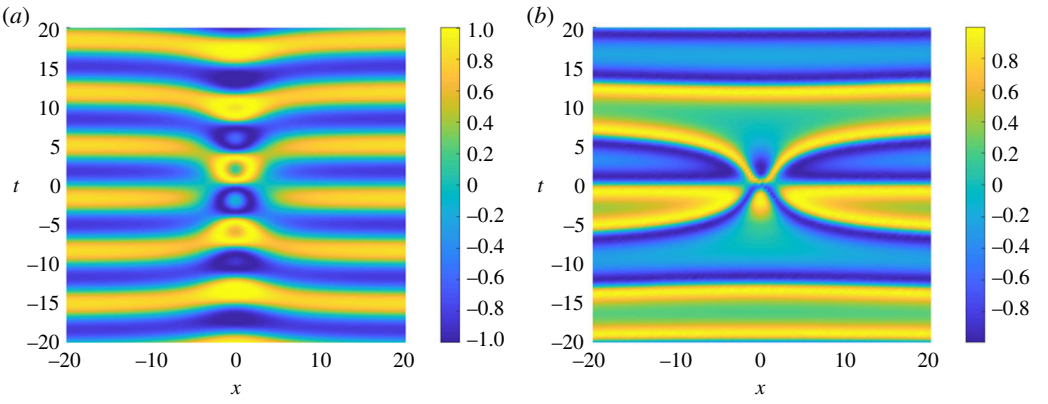

Figure 2. Surface plots of sin(u) versus (x, t) for rogue waves on the background of librational waves for $k = \sin(\frac{\pi}{6})$ (*a*) and $k = \sin(\frac{11\pi}{24})$ (*b*). (Online version in colour.)

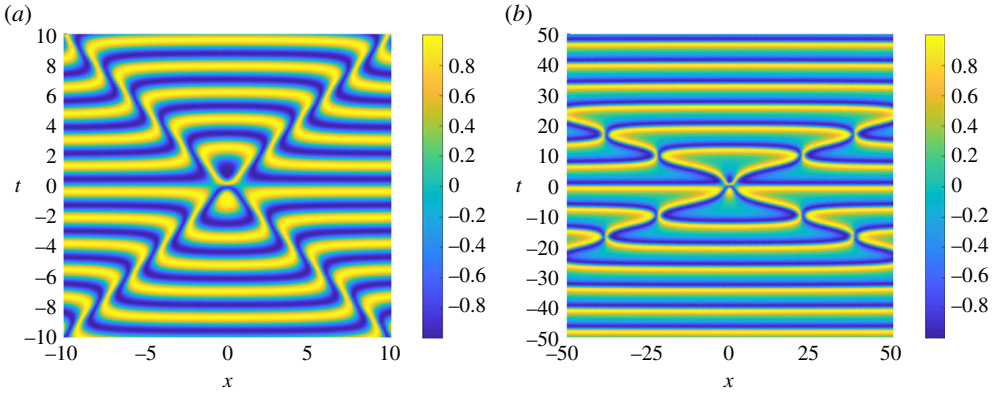

Figure 3. Surface plots of sin(u) versus (x, t) for kinks and antikinks propagating on the background of rotational waves for $k = \sin(\frac{\pi}{6})$ (*a*) and $k = \sin(\frac{11\pi}{24})$ (*b*). (Online version in colour.)

Rogue waves on the background of librational waves are displayed in figure 2, where surface plots of sin(u) are plotted versus (x, t). The wave patterns are very similar to the solutions from appendix D of [3] or the rogue wave observed on figure 1*a* (left). This confirms that rogue waves on a background of librational waves model defects in the fluxon condensate obtained in [3] from the Riemann–Hilbert problem.

Kinks and antikinks propagating on the background of rotational waves are shown in figure 3, where the surface plots of sin(u) are plotted versus (x, t). The wave patterns appear very similar to the propagation of kinks and antikinks seen in figure 1*b* (left) in the dynamics of the fluxon condensate in the semi-classical limit [1,2].

This article is organized as follows. Travelling periodic waves of the sine-Gordon equation are expressed by elliptic functions in §2. Lax equations are introduced for the sine-Gordon equation in characteristic variables in §3. The algebraic method is developed in §4, where the bounded periodic eigenfunctions in space–time coordinates are explicitly computed for particular eigenvalues in the Lax spectrum. The new solutions on the background of the rotational (librational) waves are constructed in §5 (§6). Section 7 concludes the paper with the summary.

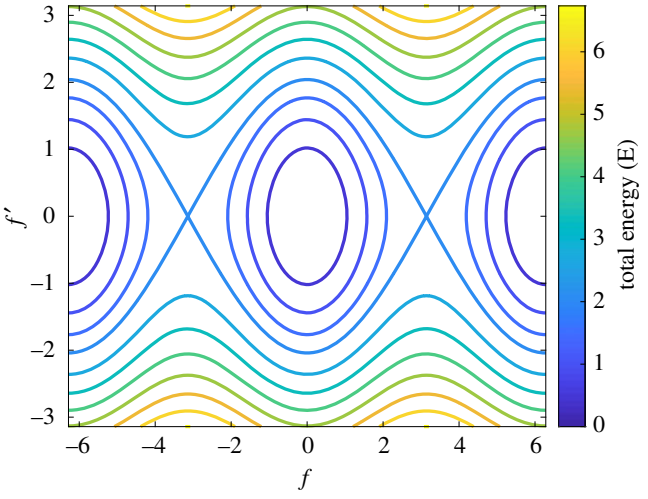

Figure 4. Orbits of the second-order equation (2.2) on the phase plane (f, f'). (Online version in colour.)

2. Travelling periodic waves

Travelling wave solutions of the sine-Gordon equation (1.3) are written in the form $u(x,t) = f(x-ct)$, where c is the wave speed and $f(x): \mathbb{R} \to \mathbb{R}$ is the wave profile satisfying the following differential equation:

$$(c^2-1)f'' + \sin(f) = 0, \tag{2.1}$$

where the prime corresponds to differentiation in x (after translation to the right by ct). Superluminal motion corresponds to $c^2 > 1$, in which case the following transformation $f(x) = \hat{f}(\hat{x})$ with $\hat{x} = x/\sqrt{c^2-1}$ results in the dimensionless equation:

$$\hat{f}'' + \sin(\hat{f}) = 0, \tag{2.2}$$

where the prime now corresponds to differentiation in $\hat{x}$. In what follows, we drop hats for simplicity of notations.

The reason why the travelling wave solutions to the sine-Gordon equation (1.3) can be expressed without the wave speed c is the following Lorentz transformation for $c^2 > 1$ (a similar transformation exists for $c^2 < 1$):

$$\hat{x} = \frac{x-ct}{\sqrt{c^2-1}}, \quad \hat{t} = \frac{t-cx}{\sqrt{c^2-1}}, \quad \hat{u} = \pi + u, \tag{2.3}$$

where $\hat{u} = \hat{u}(\hat{x},\hat{t})$ satisfies the same sine-Gordon equation (1.3). The time-independent function $\hat{u}(\hat{x},\hat{t}) = \pi + \hat{f}(\hat{x})$ satisfies the differential equation (2.2).

The second-order equation (2.2), where hats are now dropped, is integrable with the first-order invariant:

$$E(f,f') := \tfrac{1}{2}(f')^2 + 1 - \cos(f). \tag{2.4}$$

It is straightforward to verify that $E(f,f')$ is constant in x along the solutions of the second-order equation (2.2). The level sets of $E(f,f')$ represent all solutions to the differential equation (2.2) as orbits on the phase plane (f,f'). Figure 4 plots the level sets of $E(f,f')$. There are three different cases for $f \in [-\pi,\pi]$. When $E \in (0,2)$, the level curve is a periodic orbit centred around $(0,0)$, which corresponds to librational motion. When $E = 2$, there are two heteroclinic orbits connecting $(-\pi,0)$ to $(\pi,0)$ which are referred to as kinks and antikinks depending on the sign of f'. Orbits for $E > 2$ yield rotational motion.

Exact analytical solutions for the librational and rotational waves are available in terms of Jacobi elliptic functions sn, cn and dn. These elliptic functions are derived from the inversion of the elliptic integral of the first kind

$$z = F(\tau, k) = \int_0^\tau \frac{\mathrm{d}t}{\sqrt{1 - k^2 \sin^2 t}},$$

where $k \in (0, 1)$ is the elliptic modulus. The complete elliptic integral is defined as $K(k) = F(\frac{\pi}{2}, k)$. The first two Jacobi elliptic functions are defined by $\mathrm{sn}(z, k) = \sin\tau$ and $\mathrm{cn}(z, k) = \cos\tau$ such that

$$\mathrm{sn}^2(z, k) + \mathrm{cn}^2(z, k) = 1. \tag{2.5}$$

These functions are smooth, sign-indefinite and periodic with the period $4K(k)$. The third Jacobi elliptic function is defined from the quadratic formula

$$\mathrm{dn}^2(z, k) + k^2 \mathrm{sn}^2(z, k) = 1. \tag{2.6}$$

The function $\mathrm{dn}(z, k)$ is given by the positive square root of (2.6), so that it is smooth, positive and periodic with the period $2K(k)$. The Jacobi elliptic functions are related by the derivatives:

$$\left.\begin{aligned} \frac{\mathrm{d}}{\mathrm{d}z}\,\mathrm{sn}(z, k) &= \mathrm{cn}(z, k)\,\mathrm{dn}(z, k), \\ \frac{\mathrm{d}}{\mathrm{d}z}\,\mathrm{cn}(z, k) &= -\mathrm{sn}(z, k)\,\mathrm{dn}(z, k), \\ \frac{\mathrm{d}}{\mathrm{d}z}\,\mathrm{dn}(z, k) &= -k^2 \mathrm{sn}(z, k)\,\mathrm{cn}(z, k). \end{aligned}\right\} \tag{2.7}$$

For $E \in (0, 2)$, the librational waves of the first-order invariant (2.4) are given up to an arbitrary translation in x by

$$\left.\begin{aligned} \cos(f) &= 1 - 2k^2 \mathrm{sn}^2(x, k), \\ \sin(f) &= 2k\,\mathrm{sn}(x, k)\mathrm{dn}(x, k) \\ f' &= 2k\,\mathrm{cn}(x, k), \end{aligned}\right\} \tag{2.8}$$

where $E = 2k^2 \in (0, 2)$. In order to verify the validity of (2.8), we note that the first-order invariant (2.4) is satisfied due to (2.5), the trigonometric identity is satisfied due to (2.6), and the derivative of $\cos(f)$ and $\sin(f)$ are consistent due to (2.7). The period of the librational waves (2.8) is $L = 4K(k)$.

For $E \in (2, \infty)$, the rotational waves of the first-order invariant (2.4) are given up to an arbitrary translation in x by

$$\left.\begin{aligned} \cos(f) &= 1 - 2\mathrm{sn}^2(k^{-1}x, k), \\ \sin(f) &= \pm 2\mathrm{sn}(k^{-1}x, k)\mathrm{cn}(k^{-1}x, k) \\ f' &= \pm 2k^{-1}\mathrm{dn}(k^{-1}x, k), \end{aligned}\right\} \tag{2.9}$$

where $E = 2k^{-2} \in (2, \infty)$ and the upper/lower sign corresponds to the orbit in the upper/lower half plane in figure 4. Again, the first-order invariant (2.4) is satisfied due to (2.6), the trigonometric identity is satisfied due to (2.5), and the derivative of $\cos(f)$ and $\sin(f)$ are consistent due to (2.7). The period of the rotational waves (2.9) is $L = 2kK(k)$.

3. Lax equations in characteristic coordinates

Lax equations for the sine-Gordon equation (1.3) are rather cumbersome [2,10]. Therefore, we adopt the following characteristic coordinates:

$$\xi = \tfrac{1}{2}(x + t) \quad \text{and} \quad \eta = \tfrac{1}{2}(x - t). \tag{3.1}$$

The sine-Gordon equation (1.3) can be written in a simpler form:

$$u_{\xi\eta} = \sin(u), \tag{3.2}$$

where $u = u(\xi, \eta)$. The travelling periodic wave is now given by $u(\xi, \eta) = \hat{f}(\xi - \eta)$, where $\hat{f}(\xi) : \mathbb{R} \to \mathbb{R}$ satisfies the second-order equation (2.2), with the prime representing the derivative with respect to $\hat{x} = \xi - \eta = t$. Note that t and $\hat{x}$ are equivalent due to the Lorenz transformation (2.3).

Lax equations for the sine-Gordon equation in characteristic coordinates (3.2) are given by the following system:

$$\frac{\partial}{\partial \xi} \begin{bmatrix} p \\ q \end{bmatrix} = \frac{1}{2} \begin{bmatrix} \lambda & -u_\xi \\ u_\xi & -\lambda \end{bmatrix} \begin{bmatrix} p \\ q \end{bmatrix} \tag{3.3}$$

and

$$\frac{\partial}{\partial \eta} \begin{bmatrix} p \\ q \end{bmatrix} = \frac{1}{2\lambda} \begin{bmatrix} \cos(u) & \sin(u) \\ \sin(u) & -\cos(u) \end{bmatrix} \begin{bmatrix} p \\ q \end{bmatrix}, \tag{3.4}$$

where $\lambda \in \mathbb{C}$ is the spectral parameter and $\chi := (p, q)^T$ is an eigenfunction written in variables (ξ, η). Validity of the sine-Gordon equation (3.2) as the compatibility condition $\chi_{\xi\eta} = \chi_{\eta\xi}$ can be checked by direct differentiation [21]. The first equation (3.3) is referred to as the AKNS spectral problem with the potential $w := -u_\xi$.

When $w = -\hat{f}'(\hat{x})$ is a travelling periodic wave with the fundamental period L, the AKNS spectral problem determines the Lax spectrum in $L^2(\mathbb{R})$ as the set of all admissible values of λ for which $\chi \in L^\infty(\mathbb{R})$. By the Floquet theorem, bounded solutions of the linear equation (3.3) can be represented in the form

$$\chi(\xi, \eta) = \phi(\xi - \eta)\, \mathrm{e}^{\mathrm{i}\mu(\xi - \eta) + \Omega\eta}, \tag{3.5}$$

where ϕ is L-periodic, μ is defined in the fundamental region $[-\frac{\pi}{L}, \frac{\pi}{L}]$ and Ω is a new spectral parameter arising in the separation of variables in the second Lax equation (3.4). The admissible values of λ in $\mathbb{C}$ are defined by periodic solutions of the following eigenvalue problem:

$$\begin{bmatrix} 2\dfrac{\mathrm{d}}{\mathrm{d}\hat{x}} + 2\mathrm{i}\mu & \hat{f}'(\hat{x}) \\ \hat{f}'(\hat{x}) & -2\dfrac{\mathrm{d}}{\mathrm{d}\hat{x}} - 2\mathrm{i}\mu \end{bmatrix} \phi = \lambda\phi, \tag{3.6}$$

where $\hat{x} := \xi - \eta$ and $\mu \in [-\frac{\pi}{L}, \frac{\pi}{L}]$. The spectral parameter Ω determines an eigenvalue of the spectral stability problem for the travelling periodic wave evolving with respect to the coordinate η (see theorem 5.1 in [10] for spectral stability of the travelling periodic wave evolving with respect to the time variable t). Compared with [10], we will not explore the spectral stability of travelling periodic waves but will construct solutions to the Lax equations (3.3) and (3.4) that correspond to $\Omega = 0$. Such eigenfunctions χ are bounded in both ξ and η, hence in the space–time coordinates (x, t).

4. Algebraic method

The purpose of the algebraic method is to find relationships between solutions of the nonlinear integrable equation and solutions of the associated linear Lax equations in order to obtain an explicit expression for the particular eigenvalues of the Lax spectrum. These eigenvalues correspond to bounded eigenfunctions in the space–time coordinates. Our presentation of the algebraic method follows closely to [13,14] devoted to the mKdV equation because the AKNS spectral problem (3.3) is identical with the potential $w(\hat{x}) := -\hat{f}'(\hat{x})$, where $\hat{x} = \xi - \eta = t$. As previously mentioned, we will drop hats for the simplicity of notations.

Assume that (p_1, q_1) is a solution to the AKNS spectral problem (3.3) for a fixed value of $\lambda = \lambda_1$. Assume that the solution $u = u(\xi, \eta)$ to the sine-Gordon equation (3.2) is related to the squared

eigenfunctions by

$$-u_\xi = p_1^2 + q_1^2. \tag{4.1}$$

The linear equation (3.3) with the constraint (4.1) becomes a nonlinear Hamiltonian system with Hamiltonian

$$H(p_1, q_1) = \lambda_1 p_1 q_1 + \tfrac{1}{4}(p_1^2 + q_1^2)^2, \tag{4.2}$$

so that

$$\frac{\partial}{\partial \xi}\begin{bmatrix} p_1 \\ q_1 \end{bmatrix} = \frac{1}{2}\begin{bmatrix} 0 & 1 \\ -1 & 0 \end{bmatrix}\begin{bmatrix} \dfrac{\partial H}{\partial p_1} \\ \dfrac{\partial H}{\partial q_1} \end{bmatrix}. \tag{4.3}$$

Let us denote the constant value of $H(p_1, q_1)$ at the solutions of (4.3) by H_0 so that

$$\lambda_1 p_1 q_1 = H_0 - \tfrac{1}{4}(f')^2. \tag{4.4}$$

Recall that $u(\xi, \eta) = f(x)$ solves the second-order equation

$$f'' + \sin(f) = 0, \tag{4.5}$$

derivative of which yields

$$f''' + \cos(f) f' = 0. \tag{4.6}$$

Comparing (4.6) with (2.4) and eliminating $\cos(f)$ produces the third-order equation

$$f''' = f'(E - 1) - \tfrac{1}{2}(f')^3, \tag{4.7}$$

where E is constant.

Differentiating the constraint (4.1) twice and using (4.3) gives

$$-f'' = \lambda_1 (p_1^2 - q_1^2) \tag{4.8}$$

and

$$f''' = \lambda_1^2 f' + 2\lambda_1 f' p_1 q_1. \tag{4.9}$$

Substituting (4.4) for $\lambda_1 p_1 q_1$ into (4.9) yields

$$f''' = \lambda_1^2 f' + 2H_0 f' - \tfrac{1}{2}(f')^3. \tag{4.10}$$

Comparing (4.10) with (4.7) gives the following relation:

$$E = \lambda_1^2 + 2H_0 + 1. \tag{4.11}$$

In order to determine the explicit formula for λ_1 in terms of E, we shall integrate the nonlinear system (4.3) by using the Lax equation:

$$2\frac{\partial}{\partial \xi} W(\lambda) = Q(\lambda) W(\lambda) - W(\lambda) Q(\lambda), \tag{4.12}$$

where

$$Q(\lambda) = \begin{bmatrix} \lambda & p_1^2 + q_1^2 \\ -p_1^2 - q_1^2 & -\lambda \end{bmatrix}, \quad W(\lambda) = \begin{bmatrix} W_{11}(\lambda) & W_{12}(\lambda) \\ W_{12}(-\lambda) & -W_{11}(-\lambda) \end{bmatrix} \tag{4.13}$$

with

$$W_{11}(\lambda) = 1 - \frac{p_1 q_1}{\lambda - \lambda_1} + \frac{p_1 q_1}{\lambda + \lambda_1} \quad \text{and} \quad W_{12}(\lambda) = \frac{p_1^2}{\lambda - \lambda_1} + \frac{q_1^2}{\lambda + \lambda_1}. \tag{4.14}$$

Substituting (4.1), (4.4) and (4.8) into (4.14) yields the following expressions:

$$W_{11}(\lambda) = 1 - \frac{4H_0 - (f')^2}{2(\lambda^2 - \lambda_1^2)}, \quad W_{12}(\lambda) = \frac{-\lambda f' - f''}{\lambda^2 - \lambda_1^2}. \tag{4.15}$$

The determinant of $W(\lambda)$ is computed from (4.14) as

$$\begin{aligned}\det[W(\lambda)] &= -[W_{11}(\lambda)]^2 - W_{12}(\lambda)W_{12}(-\lambda)\\ &= -1 + \frac{4\lambda_1 p_1 q_1 + (p_1^2+q_1^2)^2}{\lambda^2-\lambda_1^2}\\ &= -1 + \frac{4H_0}{\lambda^2-\lambda_1^2},\end{aligned}$$

where we have used (4.4). Hence, $\det[W(\lambda)]$ only admits simple poles at $\lambda = \pm\lambda_1$. On the other hand, the determinant of $W(\lambda)$ is computed from (4.15) as

$$\begin{aligned}\det[W(\lambda)] &= -1 + \frac{4H_0 - (f')^2}{\lambda^2-\lambda_1^2} + \frac{(\lambda^2+2H_0)(f')^2 - (f'')^2 - 4H_0^2 - \frac{1}{4}(f')^4}{(\lambda^2-\lambda_1^2)^2}\\ &= -1 + \frac{4H_0}{\lambda^2-\lambda_1^2} + \frac{4(\lambda_1^2+2H_0)(f')^2 - 4(f'')^2 - 16H_0^2 - (f')^4}{4(\lambda^2-\lambda_1^2)^2}.\end{aligned}$$

Comparison of these two equivalent expressions yields the constraint:

$$(\lambda_1^2+2H_0)(f')^2 - (f'')^2 - 4H_0^2 - \tfrac{1}{4}(f')^4 = 0. \tag{4.16}$$

By a fundamental trigonometric identity, we obtain from (2.4) and (4.5):

$$1 = \sin^2(f) + \cos^2(f) = (f'')^2 + \tfrac{1}{4}(f')^4 + (1-E)(f')^2 + (1-E)^2. \tag{4.17}$$

Comparing (4.16) and (4.17) yields the relation

$$4H_0^2 = E(E-2), \tag{4.18}$$

in addition to (4.11). Expressing H_0 from (4.18) and substituting into (4.11) yields admissible values of λ_1 by

$$\lambda_1^2 = E - 1 \mp \sqrt{E(E-2)}, \tag{4.19}$$

where the plus and minus sign correspond to the two roots in

$$2H_0 = \pm\sqrt{E(E-2)}. \tag{4.20}$$

For the rotational waves (2.9), we have $E = 2/k^2$, so that one can extract the square root from (4.19) and obtain two real pairs of admissible values $\pm\lambda_1$ with

$$\lambda_1 = \frac{1 \mp \sqrt{1-k^2}}{k}, \tag{4.21}$$

where the upper and lower signs correspond to the choice of signs in

$$H_0 = \pm\frac{\sqrt{1-k^2}}{k^2}. \tag{4.22}$$

For the librational waves (2.8), we have $E = 2k^2$ so that one can again extract the square root from (4.19) and obtain a complex quadruplet of admissible values $\{\pm\lambda_1, \pm\bar{\lambda}_1\}$ with

$$\lambda_1 = k + \mathrm{i}\sqrt{1-k^2}, \tag{4.23}$$

where the unique λ_1 is located in the first quadrant of the complex plane. This eigenvalue corresponds to

$$H_0 = -\mathrm{i}k\sqrt{1-k^2}. \tag{4.24}$$

We approximate numerically the Lax spectrum of the AKNS spectral problem (3.3) by using the Floquet theorem and converting the spectral problem to the form (3.6). By using discretization of the spatial domain $[0, L]$ and the range of the μ values in $[-\frac{\pi}{L}, \frac{\pi}{L}]$, we reduce (3.6) to the matrix eigenvalue problem for each μ; this problem is handled using Matlab's eig function. The derivative operator $\frac{\mathrm{d}}{\mathrm{d}\hat{x}}$ is replaced with the 12th-order finite difference matrix to ensure high

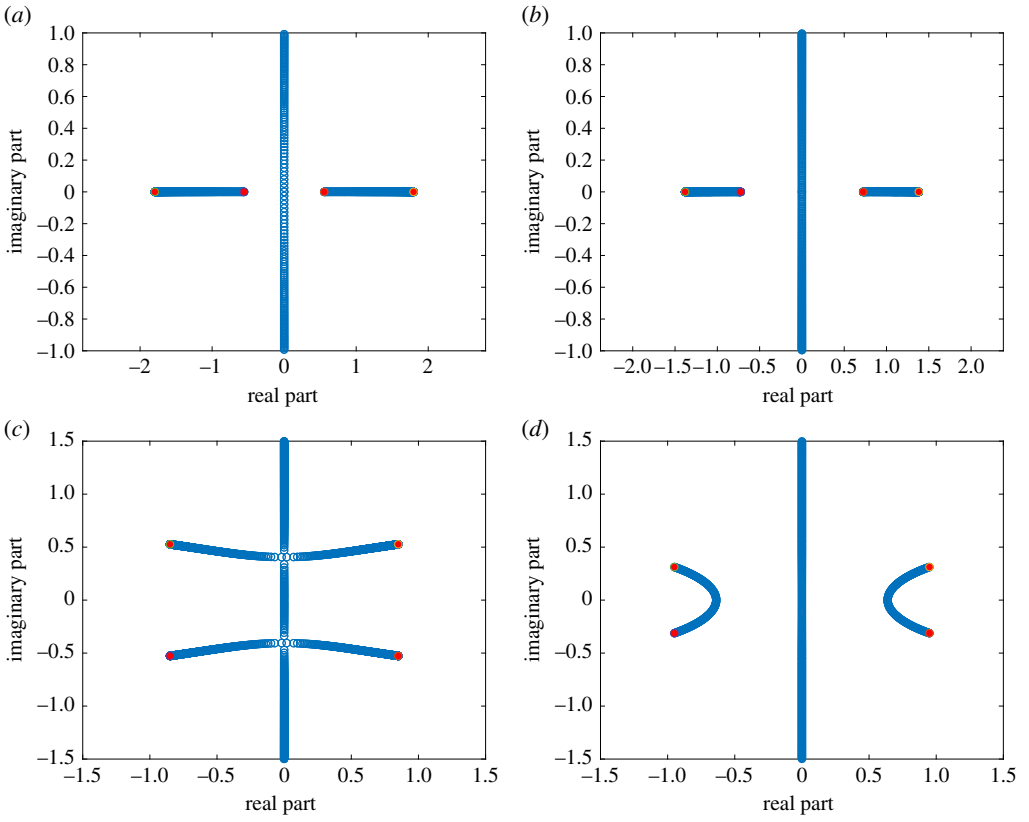

Figure 5. The Lax spectrum of (3.3) associated with the rotational (*a*,*b*) and librational (*c*,*d*) waves for $k = 0.85$ (*a*,*c*) and $k = 0.95$ (*b*,*d*). Red dots represent eigenvalues (4.21) and (4.23). (Online version in colour.)

accuracy of computations. The union of each set of eigenvalues associated for each μ defines the Lax spectrum.

Figure 5 shows the numerically constructed Lax spectra for the rotational and librational waves using certain values of k. The endpoints of the spectral bands outside $i\mathbb{R}$ shown by red dots correspond to the eigenvalues (4.21) and (4.23).

Lax spectra in figure 5 correspond to the AKNS spectral problem (3.3) for the sine-Gordon equation in characteristic variables (ξ, η). The location of the Lax spectrum in space–time coordinates (x, t) is different because the bounded eigenfunctions in ξ are located at different values of $\lambda \in \mathbb{R}$ compared with bounded functions in $x = \xi + \eta$. Nevertheless, the eigenvalues (4.21) and (4.23) belong to the Lax spectrum in (x, t) because the corresponding eigenfunctions are bounded and periodic both in x and t. The same eigenvalues are shown by crosses in fig. 7 in [10], from which it is clear that the eigenvalues (4.21) and (4.23) do not appear as the endpoints of the Lax spectrum in the space–time coordinates (x, t).

5. New solutions on the background of rotational waves

Let (p, q) be a solution to the linear equations (3.3) and (3.4) for a fixed value of λ and for the solution $u = u(\xi, \eta)$ of the sine-Gordon equation (3.2). As is shown in [13], the new solution $\hat{u} = \hat{u}(\xi, \eta)$ to the sine-Gordon equation is given by the onefold Darboux transformation:

$$\hat{w} = w + \frac{4\lambda pq}{p^2 + q^2}, \tag{5.1}$$

where $w := -u_\xi$ and $\hat{w} := -\hat{u}_\xi$. If $u = f(\xi - \eta)$ is the rotational wave given by (2.9) with $x = \xi - \eta$ and $\lambda = \lambda_1$ is given by the algebraic method with the eigenfunction $(p, q) = (p_1, q_1)$ satisfying (4.1) and (4.4), the onefold Darboux transformation (5.1) yields

$$\hat{w} = w + \frac{4\lambda_1 p_1 q_1}{p_1^2 + q_1^2} = w + \frac{4H_0 - w^2}{w} = \frac{4H_0}{w}. \tag{5.2}$$

Since $w = -f'$ is given by (2.9) and H_0 is given by (4.22), we obtain up to the sign changes:

$$\hat{w} = \pm \frac{2k^{-1}\sqrt{1-k^2}}{\mathrm{dn}(k^{-1}x; k)} = \pm 2k^{-1}\,\mathrm{dn}(k^{-1}x + K(k); k). \tag{5.3}$$

The new solution (5.3) is just a half-period translated and reflected version of the rotational wave, which is periodic with the period $L = 2kK(k)$.

In order to construct a new solution to the sine-Gordon equation on the background of the rotational wave (2.9), we are looking for the second, linear independent solution to the linear equations (3.3) and (3.4) with the same value of $\lambda = \lambda_1$. We will define the second solution in the same form as is used in [14]:

$$\hat{p}_1 = p_1\phi_R - \frac{q_1}{p_1^2 + q_1^2} \quad \text{and} \quad \hat{q}_1 = q_1\phi_R + \frac{p_1}{p_1^2 + q_1^2}, \tag{5.4}$$

where the function $\phi_R = \phi_R(\xi, \eta)$ satisfies the system of scalar equations:

$$\frac{\partial \phi_R}{\partial \xi} = -\frac{2\lambda_1 p_1 q_1}{(p_1^2 + q_1^2)^2} \quad \text{and} \quad \lambda_1 \frac{\partial \phi_R}{\partial \eta} = \frac{(p_1^2 - q_1^2)\sin(f) - 2p_1 q_1 \cos(f)}{(p_1^2 + q_1^2)^2}. \tag{5.5}$$

The representation (5.4) is non-singular for the rotational waves because $w = p_1^2 + q_1^2 = -f'$ has the sign-definite f' in (2.9). As we prove below, the exact expression for ϕ_R is given by

$$\phi_R(\xi, \eta) = C + \frac{1}{2}(\xi + \eta) - 2H_0 \int_0^{\xi - \eta} \frac{\mathrm{d}x}{(f')^2}, \tag{5.6}$$

where C is an arbitrary constant of integration. Indeed, by using (4.1), (4.4) and (4.8), we rewrite (5.5) in the form:

$$\frac{\partial \phi_R}{\partial \xi} = \frac{1}{2} - \frac{2H_0}{(f')^2} \quad \text{and} \quad \lambda_1^2 \frac{\partial \phi_R}{\partial \eta} = -\frac{2f''\sin(f) + (4H_0 - (f')^2)\cos(f)}{2(f')^2}. \tag{5.7}$$

By using (2.4), (4.5), (4.11) and (4.16), the second equation of system (5.7) is simplified to

$$\frac{\partial \phi_R}{\partial \eta} = \frac{1}{2} + \frac{2H_0}{(f')^2}, \tag{5.8}$$

which implies (5.6) due to the first equation of system (5.7) and $f = f(\xi - \eta)$.

If f and (p_1, q_1) are L-periodic functions in $x := \xi - \eta$ with period $L = 2kK(k)$, the function ϕ_R and $(\hat{p}_1, \hat{q}_1)$ are non-periodic. When the second, linearly independent solution $(p, q) = (\hat{p}_1, \hat{q}_1)$ is used in the onefold Darboux transformation (5.1), it generates a new solution with an algebraic structure on the background of the rotational waves. The new solution approaches the rotational wave along the directions in the (ξ, η) plane where $|\phi_R|$ grows to infinity.

We recall (2.9) and (5.3) to rewrite (5.6) in the equivalent form:

$$\phi_R(\xi, \eta) = C + \frac{1}{2}(\xi + \eta) - \frac{H_0 k^3}{2(1-k^2)} \int_0^{k^{-1}(\xi - \eta)} \mathrm{dn}^2(z + K(k); k)\,\mathrm{d}z. \tag{5.9}$$

Also recall the complete elliptic integral of the second kind

$$E(k) = \int_0^{K(k)} \mathrm{dn}^2(z; k)\,\mathrm{d}k.$$

Over the period $L = 2kK(k)$, the integral in (5.9) is incremented by $2E(k)$, hence $|\phi_R(\xi,\eta)| \to \infty$ along every direction in the (ξ,η)-plane with the exception of the direction of the straight line:

$$\Omega := \left\{ (\xi,\eta) \in \mathbb{R}^2 : \quad (\xi+\eta) - \frac{H_0 k^2 E(k)}{(1-k^2)K(k)}(\xi-\eta) = 0 \right\}. \tag{5.10}$$

The integration constant C serves as a parameter that translates the straight line Ω in the (ξ,η)-plane within the period of the rotational wave.

Let us now take the onefold Darboux transformation (5.1) with the second linearly independent solution (5.4) for the admissible eigenvalues λ_1 given by (4.21). By using the relations (4.1), (4.4) and (4.8), we obtain

$$\begin{aligned} \hat{w} &= w + \frac{4\lambda_1 \hat{p}_1 \hat{q}_1}{\hat{p}_1^2 + \hat{q}_1^2} \\ &= w + \frac{4\lambda_1 [p_1 q_1 (\phi_R^2 w^2 - 1) + \phi_R w (p_1^2 - q_1^2)]}{(p_1^2 + q_1^2)(\phi_R^2 w^2 + 1)} \\ &= w + \frac{(4H_0 - w^2)(\phi_R^2 w^2 - 1) + 4\phi_R w \partial_\xi w}{w(\phi_R^2 w^2 + 1)}, \end{aligned} \tag{5.11}$$

where $\hat{w} = -\hat{u}_\xi$ and $w = -u_\xi$.

We show next that the new solution (5.11) describes a kink propagating on the background of the rotational wave. Indeed, the function $\phi_R(\xi,\eta) : \mathbb{R}^2 \mapsto \mathbb{R}$ is bounded and periodic in the direction of the line Ω given by (5.10). In every other direction on the (ξ,η)-plane, $|\phi_R(\xi,\eta)| \to \infty$ so that the new solution (5.11) satisfies the limit:

$$\lim_{|\phi_R| \to \infty} \hat{w} = w + \frac{4H_0 - w^2}{w} = \frac{4H_0}{w}, \tag{5.12}$$

which coincides with (5.2). As follows from (5.3), this limit is a half-period translated and reflected version of the rotational wave. Since the divergence of $|\phi_R(\xi,\eta)| \to \infty$ is linear in (ξ,η) as follows from (5.9), the new solution (5.11) approaches the translated and reflected rotational wave algebraically fast.

Along the direction Ω, the new solution (5.11) does not approach the rotational wave. It follows from (5.11) at the critical point of $w = -f'$, where $\partial_\xi w = -f''$ is zero, that the maximum of $|\hat{w}|$ happens at the points, where $\phi_R = 0$ and

$$\hat{w}|_{\phi_R = 0} = w - \frac{4H_0 - w^2}{w} = 2w - \frac{4H_0}{w}. \tag{5.13}$$

Compared with the maximum of the rotational wave $\sup_{(\xi,\eta)\in\mathbb{R}^2} |w(\xi,\eta)| = 2k^{-1}$, the maximum of the new solution (5.11) is attained at $\sup_{(\xi,\eta)\in\mathbb{R}^2} |\hat{w}(\xi,\eta)| = 2k^{-1}M$, where M is the magnification factor given by

$$M(k) = 2 \mp \sqrt{1-k^2}. \tag{5.14}$$

The sign choice in (5.14) corresponds to the sign choice in (4.21) and (4.22). The magnification factor M determines the maximum of the localized wave propagating on the background of the rotational waves in the direction of the straight line Ω. The position of the localized wave is changed by the parameter C for the integration constant. The localized wave is greater for the lower sign in (4.21) and (4.22). Note that the magnification factor in (5.14) was previously derived for similar solutions to the NLS and mKdV equations in [13,15].

Figure 6 illustrates the exact solution (5.11) for $k = 0.95$ and two sign choices in (4.21). The value of C is set to 0 in (5.9). It follows that the solution surface of $|\hat{w}(\xi,\eta)|$ achieves its maximum at $(\xi,\eta) = (0,0)$ and is repeated along the direction of Ω. This is the direction of propagation of the localized wave on the background of the rotational waves. The localized wave has a bigger magnification for the larger value of λ_1 (figure 6*b*) and smaller magnification for the smaller value of λ_1 (figure 6*a*).

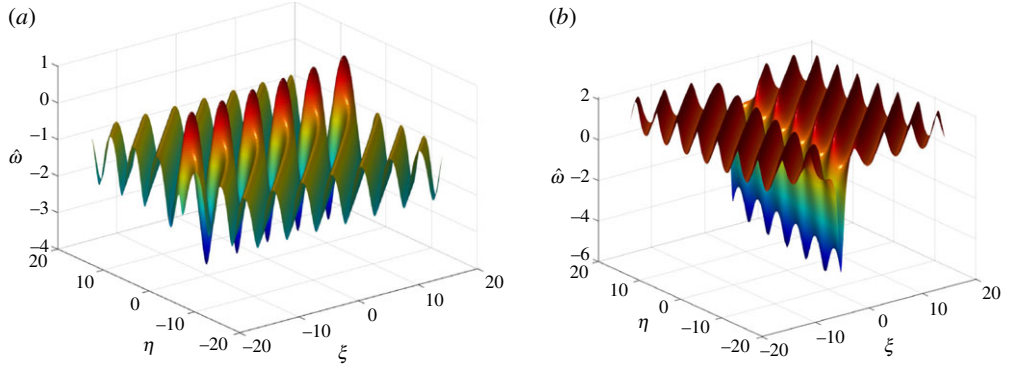

Figure 6. Localized waves on the rotational wave with $k = 0.95$ generated from the onefold Darboux transformation using eigenvalues (4.21) with the upper (*a*) and lower (*b*) signs. (Online version in colour.)

The kink and antikink in figure 6 propagate into opposite directions for the different sign choices of λ_1 in (4.21). Indeed, it follows from (4.22) and (5.10) in variables (x, t) that the kink and antikink propagate along the straight lines

$$x = \pm \frac{E(k)}{\sqrt{1-k^2}K(k)} t, \tag{5.15}$$

hence the propagation directions are opposite to each other. Since $E(k) > \sqrt{1-k^2}K(k)$, the speed of propagation exceeds one, hence these solutions are relevant for the superluminal dynamics of the sine-Gordon equation (1.3).

Kink and antikinks can be added together on the background of the rotational wave using the twofold Darboux transformation. Let (p_1, q_1) and (p_2, q_2) be solutions to the linear equations (3.3) and (3.4) with fixed values of $\lambda = \lambda_1$ and $\lambda = \lambda_2$ such that $\lambda_1 \neq \pm\lambda_2$. As is shown in [13], the twofold Darboux transformation takes the form:

$$\hat{w} = w + \frac{4(\lambda_1^2 - \lambda_2^2)[\lambda_1 p_1 q_1 (p_2^2 + q_2^2) - \lambda_2 p_2 q_2 (p_1^2 + q_1^2)]}{(\lambda_1^2 + \lambda_2^2)(p_1^2 + q_1^2)(p_2^2 + q_2^2) - 2\lambda_1\lambda_2[4p_1 q_1 p_2 q_2 + (p_1^2 - q_1^2)(p_2^2 - q_2^2)]}, \tag{5.16}$$

where $w := -u_\xi$ and $\hat{w} := -\hat{u}_\xi$. Figure 7 illustrates the exact solution obtained from (5.16) with λ_1 and λ_2 given by (4.21) for different sign choices. We have computed $\sin(\hat{u}) = \hat{u}_{\xi\eta}$ by numerically differentiating $\hat{w} = -\hat{u}_\xi$ in η with a forward difference. The corresponding surface plots of $\sin(\hat{u})$ in (x, t) are presented in figure 3.

6. New solutions on the background of librational waves

If the new solution $\hat{u} = \hat{u}(\xi, \eta)$ to the sine-Gordon equation (3.2) is given by the onefold Darboux transformation (5.11) and $u = u(\xi, \eta)$ is the librational wave, then $\hat{u}$ is no longer real-valued because H_0 and λ_1 are complex-valued in (4.23) and (4.24). The twofold Darboux transformation (5.16) is required to generate new real-valued solutions on the background of the librational waves. We take λ_1 and H_0 as in (4.23) and (4.24), and define $\lambda_2 = \bar{\lambda}_1$ with $p_2 = \bar{p}_1$ and $q_2 = \bar{q}_1$. By using (4.1), (4.4), (4.8) and (4.16), we obtain from (5.16):

$$\hat{w} = w + \frac{4(\lambda_1^2 - \bar{\lambda}_1^2)(H_0 - \bar{H}_0)w}{(\lambda_1^2 + \bar{\lambda}_1^2)w^2 - 2[-4H_0^2 + \frac{1}{4}w^4 + (w')^2]} = -w. \tag{6.1}$$

The new solution (6.1) is simply a reflected version of the librational wave. Therefore, we are looking for the second, linearly independent solution to the linear equations (3.3) and (3.4) for the same value of λ_1. One representation for the second solution is given by (5.4). However, $w = p_1^2 + q_1^2 = -f'$ crosses zero for librational waves, hence the representation (5.4) becomes singular

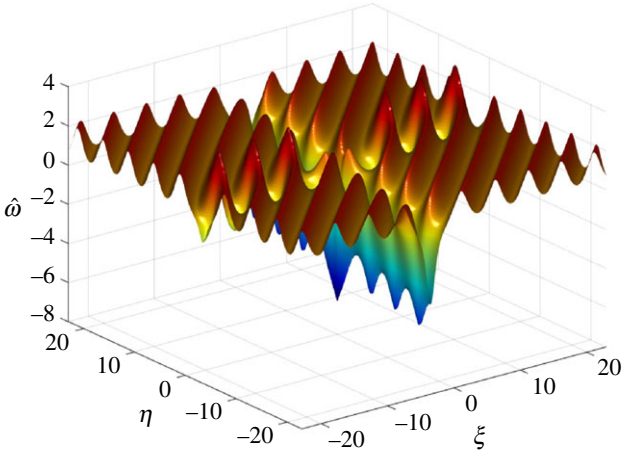

Figure 7. Localized waves on the rotational wave with $k = 0.95$ generated from the twofold Darboux transformation using both the eigenvalues (4.21) with the upper and lower signs. (Online version in colour.)

at some points. For librational waves, we should define the second solutions in a different form used in [13]:

$$\hat{p}_1 = \frac{\phi_L - 1}{q_1} \quad \text{and} \quad \hat{q}_1 = \frac{\phi_L + 1}{p_1}, \tag{6.2}$$

where the function $\phi_L = \phi_L(\xi, \eta)$ satisfies the system of scalar equations:

$$\frac{\partial \phi_L}{\partial \xi} = \frac{f'(p_1^2 - q_1^2)}{2p_1 q_1}\phi_L - \frac{f'(p_1^2 + q_1^2)}{2p_1 q_1} \quad \text{and} \quad \lambda_1 \frac{\partial \phi_L}{\partial \eta} = \frac{(p_1^2 + q_1^2)\sin(f)}{2p_1 q_1}\phi_L - \frac{(p_1^2 - q_1^2)\sin(f)}{2p_1 q_1}. \tag{6.3}$$

The representation (6.2) is non-singular because if either p_1 or q_1 vanish in some points, then equations (4.1) and (4.8) yield a contradiction with real f and complex λ_1. As we prove below, the exact expression for ϕ_L is given by

$$\phi_L(\xi, \eta) = (4H_0 - (f')^2)\left(C + \frac{\eta}{2\lambda_1} + \int_0^{\xi - \eta} \frac{2\lambda_1 (f')^2 \, \mathrm{d}x}{(4H_0 - (f')^2)^2}\right), \tag{6.4}$$

where C is an arbitrary constant of integration. By substituting (4.1), (4.4) and (4.8) in (6.3), we obtain:

$$\frac{\partial \phi_L}{\partial \xi} = \frac{2f'f''}{(f')^2 - 4H_0}\phi_L - \frac{2\lambda_1 (f')^2}{(f')^2 - 4H_0} \quad \text{and} \quad \lambda_1 \frac{\partial \phi_L}{\partial \eta} = -\frac{2\lambda_1 f'f''}{(f')^2 - 4H_0}\phi_L + \frac{2(f'')^2}{(f')^2 - 4H_0}. \tag{6.5}$$

By using

$$\phi_L = (4H_0 - (f')^2)\Upsilon, \tag{6.6}$$

with $\Upsilon = \Upsilon(\xi, \eta)$, system (6.5) can be simplified to the form:

$$\frac{\partial \Upsilon}{\partial \xi} = \frac{2\lambda_1 (f')^2}{(4H_0 - (f')^2)^2} \quad \text{and} \quad \lambda_1 \frac{\partial \Upsilon}{\partial \eta} = -\frac{2(f'')^2}{(4H_0 - (f')^2)^2}. \tag{6.7}$$

If follows from (4.16) and (6.7) that

$$\frac{\partial \Upsilon}{\partial \xi} + \frac{\partial \Upsilon}{\partial \eta} = \frac{1}{2\lambda_1}, \tag{6.8}$$

which implies that

$$\Upsilon(\xi, \eta) = C + \frac{\eta}{2\lambda_1} + G(\xi - \eta), \tag{6.9}$$

for some function $G(x) : \mathbb{R} \mapsto \mathbb{C}$ to be determined. Substituting this into (6.7) yields

$$G' = \frac{2\lambda_1 (f')^2}{(4H_0 - (f')^2)^2},$$

so that integration and substitution into (6.6) and (6.9) yields (6.4).

The functions f and (p_1, q_1) are L-periodic functions with period $L = 4K(k)$ for librational waves, however, the functions ϕ_L and $(\hat{p}_1, \hat{q}_1)$ are non-periodic. We shall prove that $|\phi_L(\xi, \eta)| \to \infty$ as $|\xi| + |\eta| \to \infty$ everywhere in the (ξ, η)-plane. Indeed, by factoring out $\frac{1}{2\lambda_1}$ in the second term of equation (6.4) and by using periodicity of $4H_0 - (f')^2$, we have $|\phi_L(\xi, \eta)| \to \infty$ if and only if $|\tilde{\phi}_L(\xi, \eta)| \to \infty$, where

$$\begin{aligned}\tilde{\phi}_L(\xi, \eta) &= \eta + \int_0^{\xi - \eta} \frac{4\lambda_1^2 (f')^2}{((f')^2 - 4H_0)^2}\, \mathrm{d}x \\ &= \eta + \int_0^{\xi - \eta} \frac{4[(2k^2 - 1) + 2ik\sqrt{1 - k^2}](f')^2}{((f')^2 + 4ik\sqrt{1 - k^2})^2}\, \mathrm{d}x.\end{aligned}$$

Taking the imaginary part yields

$$\begin{aligned}\mathrm{Im}[\tilde{\phi}] &= 8k\sqrt{1 - k^2} \int_0^{\xi - \eta} \frac{(f')^4 - 4(2k^2 - 1)(f')^2 - 16k^2(1 - k^2)}{((f')^4 + 16k^2(1 - k^2))^2} (f')^2\, \mathrm{d}x \\ &= 128k^3\sqrt{1 - k^2} \int_0^{\xi - \eta} \frac{k^2 \mathrm{cn}^4(x; k) + (1 - 2k^2)\mathrm{cn}^2(x; k) + k^2 - 1}{((f')^4 + 16k^2(1 - k^2))^2} (f')^2\, \mathrm{d}x \\ &= -128k^3\sqrt{1 - k^2} \int_0^{\xi - \eta} \frac{\mathrm{sn}^2(x; k)\mathrm{dn}^2(x; k)}{((f')^4 + 16k^2(1 - k^2))^2} (f')^2\, \mathrm{d}x,\end{aligned}$$

where we have used (2.8) in order to express $f'(x) = 2k\mathrm{cn}(x; k)$ and simplify the elliptic functions. The integrand is clearly positive for every $k \in (0, 1)$. This means that $\mathrm{Im}[\tilde{\phi}]$ remains bounded only in the diagonal direction on the (ξ, η) plane, however, in this direction $\mathrm{Re}[\tilde{\phi}]$ grows linearly in η. Hence, $|\phi_L(\xi, \eta)| \to \infty$ along every direction in the (ξ, η) plane.

Let us now take the twofold Darboux transformation (5.16) with the second, linearly independent solution (6.2) to the linear equations (3.3) and (3.4) for $\lambda_1 = k + \mathrm{i}\sqrt{1 - k^2}$ and $\lambda_2 = \bar{\lambda}_1$. The new solution is written in the form:

$$\hat{w} = w + \frac{4(\lambda_1^2 - \lambda_2^2)[\lambda_1 \hat{p}_1 \hat{q}_1 (\hat{p}_2^2 + \hat{q}_2^2) - \lambda_2 \hat{p}_2 \hat{q}_2 (\hat{p}_1^2 + \hat{q}_1^2)]}{(\lambda_1^2 + \lambda_2^2)(\hat{p}_1^2 + \hat{q}_1^2)(\hat{p}_2^2 + \hat{q}_2^2) - 2\lambda_1 \lambda_2 [4\hat{p}_1 \hat{q}_1 \hat{p}_2 \hat{q}_2 + (\hat{p}_1^2 - \hat{q}_1^2)(\hat{p}_2^2 - \hat{q}_2^2)]}, \tag{6.10}$$

where $(\hat{p}_2, \hat{q}_2)$ are taken as the complex conjugate to $(\hat{p}_1, \hat{q}_1)$.

We will prove that the new solution (6.10) describes an isolated rogue wave arising on the background of the librational wave. Indeed, the function $\phi_L(\xi, \eta) : \mathbb{R}^2 \mapsto \mathbb{R}$ is unbounded in every direction on the (ξ, η) plane, so that

$$\lim_{|\phi_L| \to \infty} \hat{w} = w + \frac{4(\lambda_1^2 - \bar{\lambda}_1^2)(H_0 - \bar{H}_0)w}{(\lambda_1^2 + \bar{\lambda}_1^2)w^2 - 2[-4H_0^2 + \frac{1}{4}w^4 + (w')^2]} = -w, \tag{6.11}$$

which coincides with (6.1). The divergence of $|\phi_L(\xi, \eta)| \to \infty$ is again linear in (ξ, η) as follows from (6.4), hence the new solution (6.10) approaches the reflected librational wave algebraically.

It follows from (6.10) at the critical points of $w = -f'$, where $\partial_\xi w = -f''$ is zero, that the maximum of $|\hat{w}|$ happens at the points, where $\phi_L = 0$ and

$$\hat{w}|_{\phi_L = 0} = w - \frac{4(\lambda_1^2 - \bar{\lambda}_1^2)(H_0 - \bar{H}_0)w}{(\lambda_1^2 + \bar{\lambda}_1^2)w^2 - 2[-4H_0^2 + \frac{1}{4}w^4 + (w')^2]} = 3w. \tag{6.12}$$

Compared with the maximum of the librational wave $\sup_{(\xi,\eta) \in \mathbb{R}^2} |w(\xi, \eta)| = 2k$, the maximum of the new solution (6.10) is attained at $\sup_{(\xi,\eta) \in \mathbb{R}^2} |\hat{w}(\xi, \eta)| = 6k$, hence the rogue wave has triple magnification compared with the background wave. Note that the rogue wave (6.10) and the triple magnification factor were previously obtained for the mKdV equation in [13].

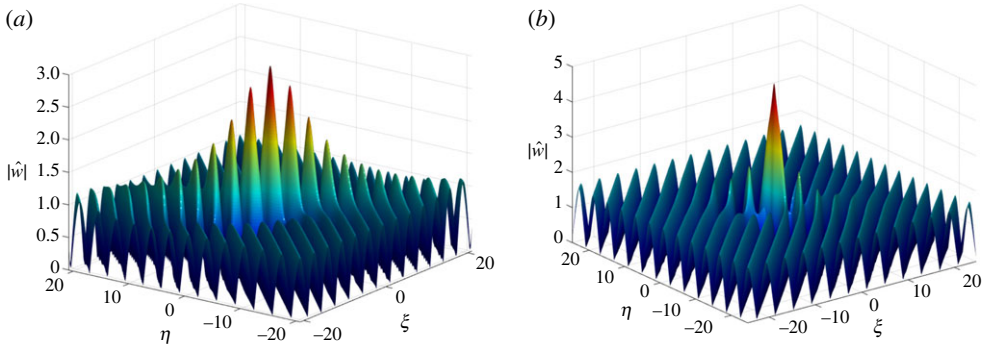

Figure 8. Rogue waves on the librational wave with $k = 0.5$ (*a*) and $k = 0.8$ (*b*). (Online version in colour.)

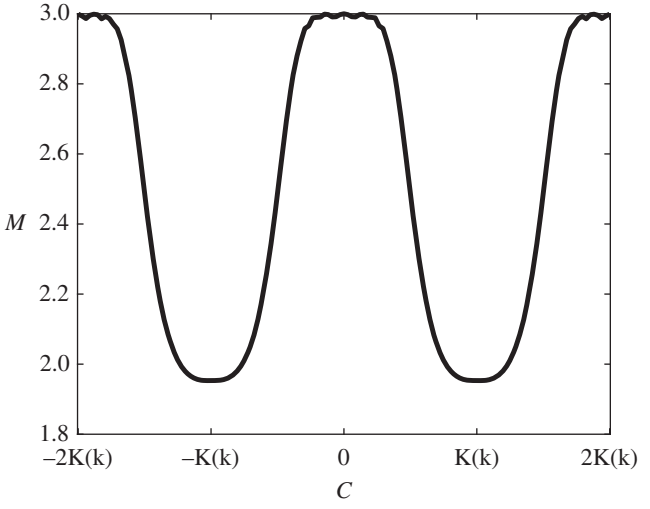

Figure 9. The magnification factor M of the rogue wave $\hat{w}$ given by (6.10) versus the constant of integration C in (6.4) for $k = 0.8$.

Figure 8 illustrates the exact solution (6.10) for two particular values of k. The value of C is set to 0 in (6.4). It is clear that the solution surface of $|\hat{w}(\xi, \eta)|$ achieves its maximum at $(\xi, \eta) = (0, 0)$ where ϕ_L vanishes. The modulus is shown for a better resolution of the oscillations of the librational wave background. Based on the same solution formula (6.10), we have computed $\sin(\hat{u}) = \hat{u}_{\xi\eta}$ by numerically differentiating $\hat{w} = -\hat{u}_\xi$ in η with a forward difference. The corresponding surface plots of $\sin(\hat{u})$ in (x, t) are presented in figure 2.

Note that the rogue wave (6.10) can be represented in a shorter form directly for $\hat{u}(\xi, \eta)$ by using another form of the Darboux transformations [20]. Moreover, higher-order Darboux transformations can be used to generate more rogue waves forming the same triangular pattern as in figure 1*a* (middle), see fig. 1 in [20]. Another representation of the same solutions follows from the Riemann–Hilbert problem, as in appendix C of [3].

Finally, we inspect how the magnification of the rogue wave depends on the constant of integration C in (6.4) and (6.10). The magnification factor is defined as

$$M := \frac{\sup_{(\xi,\eta)\in\mathbb{R}^2} |\hat{w}(\xi, \eta)|}{\sup_{(\xi,\eta)\in\mathbb{R}^2} |w(\xi, \eta)|}.$$

Figure 9 presents the plot of M versus C for $k = 0.8$. When $C = 0$, the magnification factor is maximal at $M = 3$. It is periodically continued with respect to C and it reaches the minimal value below 2. The minimal value of M depends on k.

7. Conclusion

We have presented new solutions to the sine-Gordon equation using an algebraic method and the Darboux transformations. The new solutions describe localized structures on the background of rotational and librational waves. These localized structures are obtained for the particular eigenvalues of the linear Lax equations that correspond to bounded solutions in the space–time coordinates. The Darboux transformations use the second, linearly independent solutions to the linear Lax equations that are unbounded in space–time coordinates.

For the rotational waves, the localized structure represents a kink or an antikink propagating along a straight line. It appears from infinity and goes to infinity. This outcome is related to the modulational stability of the rotational waves.

For the librational waves, the localized structure represents a rogue wave appearing from nowhere and disappearing without a trace. The rogue wave is related to the modulational instability of the librational waves.

New solutions for localized structures on the background of rotational and librational waves can be used for modelling of dynamics of the fluxon condensates. They represent the principal waveforms in the universal dynamics of the sine-Gordon equation in the semi-classical limit.

Data accessibility. MATLAB codes are publicly available in the MSc thesis [23].

Authors' contributions. R.W. performed computations and prepared figures, as part of his MSc thesis [23]. D.P. performed supervision and wrote the draft of the manuscript based on the MSc thesis. Both authors gave final approval for publication and agree to be held accountable for the work performed therein.

Competing interests. We declare we have no competing interests.

Funding. This project was supported in part by the National Natural Science Foundation of China (grant no. 11971103).

Acknowledgements. The authors thank P.D. Miller and B.Y. Lu for sharing their preprint [3] before submission and many relevant discussions. They also thank L. Ling for bringing [20] to their attention and useful remarks.

References

1. Buckingham RJ, Miller PD. 2012 The sine-Gordon equation in the semi-classical limit: critical behavior near a separatrix. *J. d'Analyse Math.* **118**, 397–492. (doi:10.1007/s11854-012-0041-3)
2. Buckingham RJ, Miller PD. 2013 The sine-Gordon equation in the semi-classical limit: dynamics of fluxon condensates. *Mem. AMS* **225**, 1–136. (doi:10.1090/S0065-9266-2012-00672-1)
3. Lu BY, Miller PD. 2019 Universality near the gradient catastrophe point in the semi-classical sine-Gordon equation. (http://arxiv.org/abs/1912.09037)
4. Scott AC, Chu FYF, Reible SA. 1976 Magnetic-flux propagation on a Josephson transmission line. *J. Appl. Phys.* **47**, 3272–3286. (doi:10.1063/1.323126)
5. Braun OM, Kivshar Yu.. 2004 *The Frenkel-Kontorova model: concepts, methods, and applications*. New York, NY: Springer.
6. Cuevas-Maraver J, Kevrekidis PG, Williams F (eds). 2014 The Sine–Gordon model and its applications. In *Nonlinear systems and complexity*, vol. 10. New York, NY: Springer.
7. Jones CKRT, Marangell R, Miller PD, Plaza RG. 2013 On the stability analysis of periodic Sine–Gordon traveling waves. *Physica D* **251**, 63–74. (doi:10.1016/j.physd.2013.02.003)
8. Jones CKRT, Marangell R, Miller PD, Plaza RG. 2014 Spectral and modulational stability of periodic wavetrains for the nonlinear Klein–Gordon equation. *J. Differ. Equ.* **257**, 4632–4703. (doi:10.1016/j.jde.2014.09.004)
9. Marangell R, Miller PD. 2015 Dynamical Hamiltonian–Hopf instabilities of periodic traveling waves in Klein–Gordon equations. *Physica D* **308**, 87–93. (doi:10.1016/j.physd.2015.06.006)
10. Deconinck B, McGill P, Segal and BL. 2017 The stability spectrum for elliptic solutions to the sine-Gordon equation. *Physica D* **360**, 17–35. (doi:10.1016/j.physd.2017.08.010)

11. Upsal J, Deconinck B. 2020 Real Lax spectrum implies spectral stability. *Stud. Appl. Math.* **145**, 765–790. (doi:10.1111/sapm.12335)
12. Clarke WA, Marangell R. 2020 A new Evans function for quasi-periodic solutions of the linearized sine-Gordon equation. (http://arxiv.org/abs/2005.08511)
13. Chen J, Pelinovsky DE. 2018 Rogue periodic waves in the modified Korteweg-de Vries equation. *Nonlinearity* **31**, 1955–1980. (doi:10.1088/1361-6544/aaa2da)
14. Chen J, Pelinovsky DE. 2019 Periodic travelling waves of the modified KdV equation and rogue waves on the periodic background. *J. Nonlin. Sci.* **29**, 2797–2843. (doi:10.1007/s00332-019-09559-y)
15. Chen J, Pelinovsky DE. 2018 Rogue periodic waves in the focusing nonlinear Schrödinger equation. *Proc. R. Soc. A* **474**, 20170814. (doi:10.1098/rspa.2017.0814)
16. Chen J, Pelinovsky DE, White RE. 2019 Rogue waves on the double-periodic background in the focusing nonlinear Schrödinger equation. *Phys. Rev. E* **100**, 052219. (doi:10.1103/PhysRevE.100.052219)
17. Chen J, Pelinovsky DE, White RE. 2020 Periodic standing waves in the focusing nonlinear Schrödinger equation: rogue waves and modulation instability. *Physica D* **405**, 132378. (doi:10.1016/j.physd.2020.132378)
18. Cao CW, Geng XG. 1990 Classical integrable systems generated through nonlinearization of eigenvalue problems. In *Nonlinear physics (Shanghai, 1989)*, pp. 68–78. Research Reports in Physics. Berlin, Germany: Springer.
19. Feng BF, Ling L, Takahashi DA. 2020 Multi-breathers and high order rogue waves for the nonlinear Schrödinger equation on the elliptic function background. *Stud. Appl. Math.* **144**, 46–101. (doi:10.1111/sapm.12287)
20. Li R, Geng X. 2020 Rogue periodic waves of the sine-Gordon equation. *Appl. Math. Lett.* **102**, 106147. (doi:10.1016/j.aml.2019.106147)
21. Ablowitz MJ, Kaup DJ, Newell AC, Segur H. 1974 The inverse scattering transform–Fourier analysis for nonlinear problems. *Stud. Appl. Math.* **53**, 249–315. (doi:10.1002/sapm1974534249)
22. Hou C, Bu L, Baronio F, Mihalache D, Chen S. 2020 Sine-Gordon breathers and formation of extreme waves in self-induced transparency media. *Rom. Rep. Phys.* **72**, 405.
23. White RE. 2020 Rogue wave potentials occurring in the sine-Gordon equation. MSc thesis, McMaster University, Hamilton, Ontario.